Arab J Geosci (2017) 10:541
https://doi.org/10.1007/s12517-017-3250-3

ORIGINAL PAPER

Exploration for iron ore in Agbado-Okudu, Kogi State, Nigeria

Nurudeen Kolawole Olasunkanmi[1] · **Olufemi S. Bamigboye**[2] · **Adebayo Aina**[1]

Received: 19 October 2016 / Accepted: 17 October 2017
© Saudi Society for Geosciences 2017

Abstract This report details the result of geophysical exploration for iron ore; which involved vertical magnetic intensity (ΔZ) and gravity measurements, to delineate the geometry and depth extent of the deposit and acquiring quantitative and qualitative information for pre-drilling purposes in Agbado-Okudu. It is located about 3 km from Jakura along Lokoja-Jakura marble quarry and within low latitude precambrian basement complex district of Kogi State, Nigeria. A total of 517 magnetic measurement points along 16 traverses and 330 gravity reading along 11 profiles on the deposit in northeast–southwest azimuth were undertaken. The magnetic and gravity data enhancement involved linear regression curve fitting and fast Fourier transform, which were used to construct residual magnetic (RM) and gravity (RG) anomalies, analytic signal amplitude, Euler deconvolution at varying spectral indices (SI), power spectrum, and source parameter image (SPI), using the submenu of Geosoft Oasis Montaj software. Interpretation of the RM and RG anomalies revealed a primary causative body which perfectly correlates the positive anomalies and iron ore deposit, in form of a horizontal or gently dipping dyke with strike length of 600 m and average width of 110–130 m, within the gneiss complex in the north and trending south of the area. A secondary causative body associated with the negative anomalies and inferred as a vertical/near vertical thin sheet striking northeast–southwest coincided with the granitic and quartzitic intrusion. The NW–SE and E–W lineament trend conformed Kibarian and Liberian orogeny cycles of generally known structural trends in Nigeria, which shows that the iron ore deposit is structurally controlled. Depths to sources were estimated within range ≤ 2–24 m and 37.5–60 m, regarded as shallow and relatively deep depths, respectively. Ten vertical boreholes ranging in depth between 50 and 100 m are recommended, five of which require a priority attention to ascertain the thickness of the primary causative body.

Keywords Iron ore deposit · Magnetic and gravity anomalies · Primary and secondary causative bodies · Dyke · Lineament · Vertical boreholes

Introduction

The quest for non-petroleum revenue and raw materials for the iron and steel industry in Nigeria presents opportunity to explore the long-abandoned Agbado-Okudu iron ore deposit. The deposit lies in the vicinity of the area marked out as anomaly 1/6 for a reconnaissance geological and geophysical survey from the data analysis of the aeromagnetic survey scale 1:50,000 carried out by the U.S.S.R. techno-export under contract 1717 of 1971/72. It was, however, not detected possibly due to the low magnetic response since the effectiveness of magnetic method depends solely on presence of magnetite in the rocks of surveyed area through delineation of associated anomalies which are usually positive and high in magnetic intensity (Oladunjoye et al. 2016). Gravity method detects and measures local variations in the densities of rocks near the surface and could be used to delineate iron ore mineralization zones from the host rock (Emerson 1990) which might not have been captured with magnetics.

Magnetic integrated with gravity data has performed noticeable role in revealing subsurface information exceptionally in geological mapping and mineral prospecting (Cericia et al. 2011; Amigun et al. 2012; Oladunjoye et al. 2016). This is

✉ Nurudeen Kolawole Olasunkanmi
nurudeen.olasunkanmi@kwasu.edu.ng; kolexy1808@gmail.com

[1] Department of Physics and Materials Science, Kwara State University, Malete, Kwara State, Nigeria

[2] Department of Geology and Mineral Science, Kwara State University, Malete, Kwara State, Nigeria

Published online: 19 December 2017

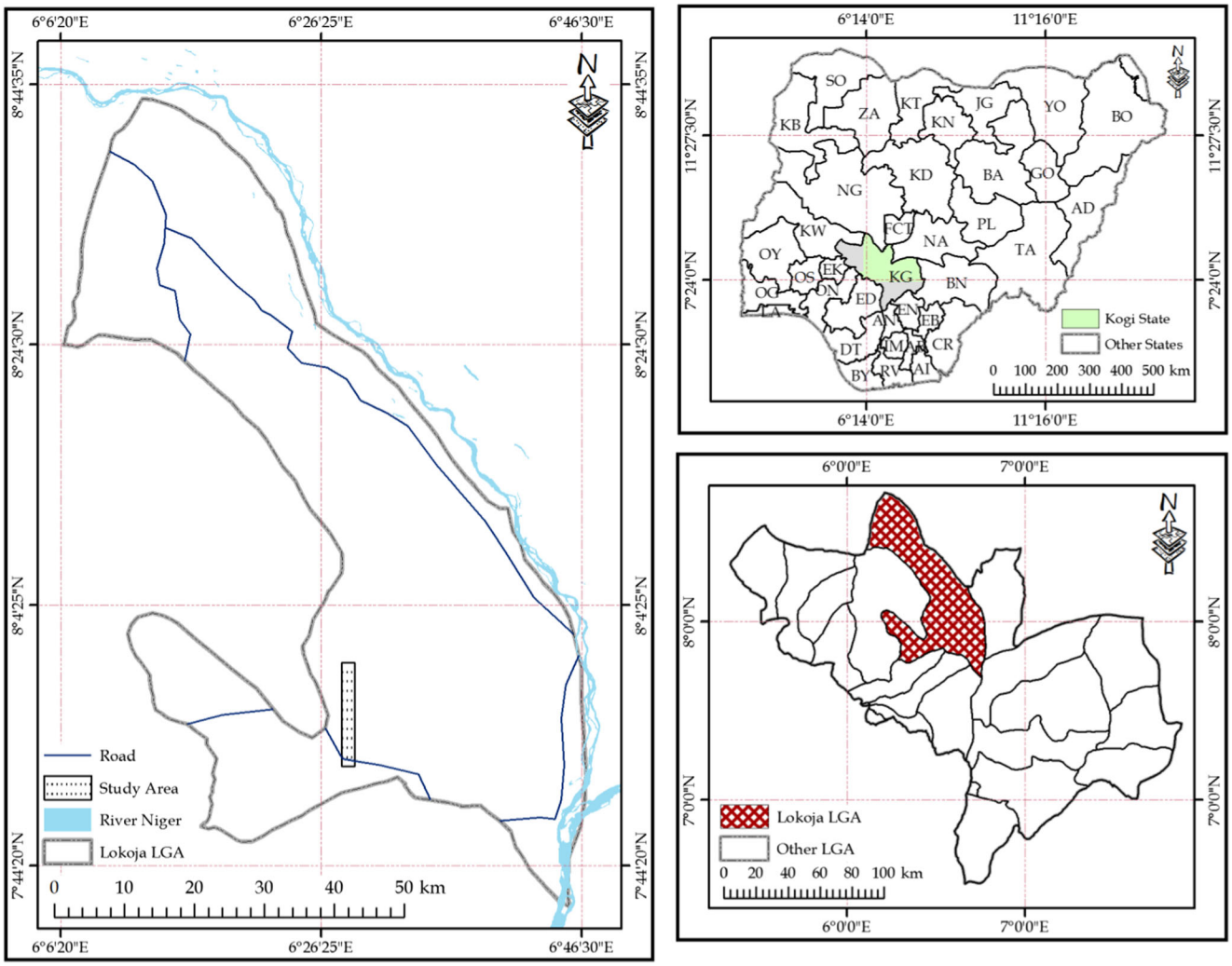


Fig. 1 Location map of the study area inset on Lokoja map, north central Nigeria

based upon the existence of measurable physical contrast associated with it (Hansen 1966; Telford et al. 1976) and several enhancement and analytical tools. Images and maps produced from the processing or enhancement tools involving Fourier filtering techniques and others such as the analytic signal, Euler deconvolution, source parameter imaging, and power spectra contribute to geological interpretation of magnetic and gravity data (Durrheim 1983; Spector and Grant 1970; Reid 1997). Fourier filtering involves transformation of potential field data (such as gravity and magnetic) to Fourier domain using fast Fourier transform and analyzing it as a function of wave number or wavelength such that features can be enhanced and the information of interest can be extracted (e.g., Foss 2011; Paananen 2013). In this study, integrated approach involving vertical magnetic and gravity anomalies analysis using fast Fourier transform on submenu of Geosoft Oasis Montaj 6.4.2 (HJ) software has been applied to delineate structural features related to faults and other lateral changes or geological contacts associated with iron ore occurrence in Agbado-Okudu.

Geology of the area

The deposit is located within longitude 6° 28′ 12″ E to 6° 28′ 23″ E and latitudes 7° 52′ 29″ to 8° 00′ 39″ N on Ayegunle Sheet 226 SE and Kabba Sheet 246 NE. It is about 1.6–2.1 km offset from Lokoja-Jakura Marble Quarry Road at about 40.7 km from Lokoja (Fig. 1); the isolated ridge on which the ore outcropped can be accessed by an exploratory track. The highest point of the ridge has a spot height of 382.65 m, and the lowest point is 216.49-m high with thickly wooded to derived savannah vegetation. It falls within the basement complex of Nigeria (Rahaman 1989: Obaje 2009), which host ferruginous quartzites that are restricted to the crest of the isolated ridge with a strike roughly N–S. It is bounded in the East by muscovite schist and gneisses and muscovite schist in the west. The gneisses are mainly restricted to the flanks of the ridge constituting a break-in-slope with a sharp drop in elevation to the foot of the ridge where the muscovite schist outcropped though sparingly and highly weathered. In situ outcrops strike and dip measurements are rather scarce; however, an average dip of 18°–30° northeast

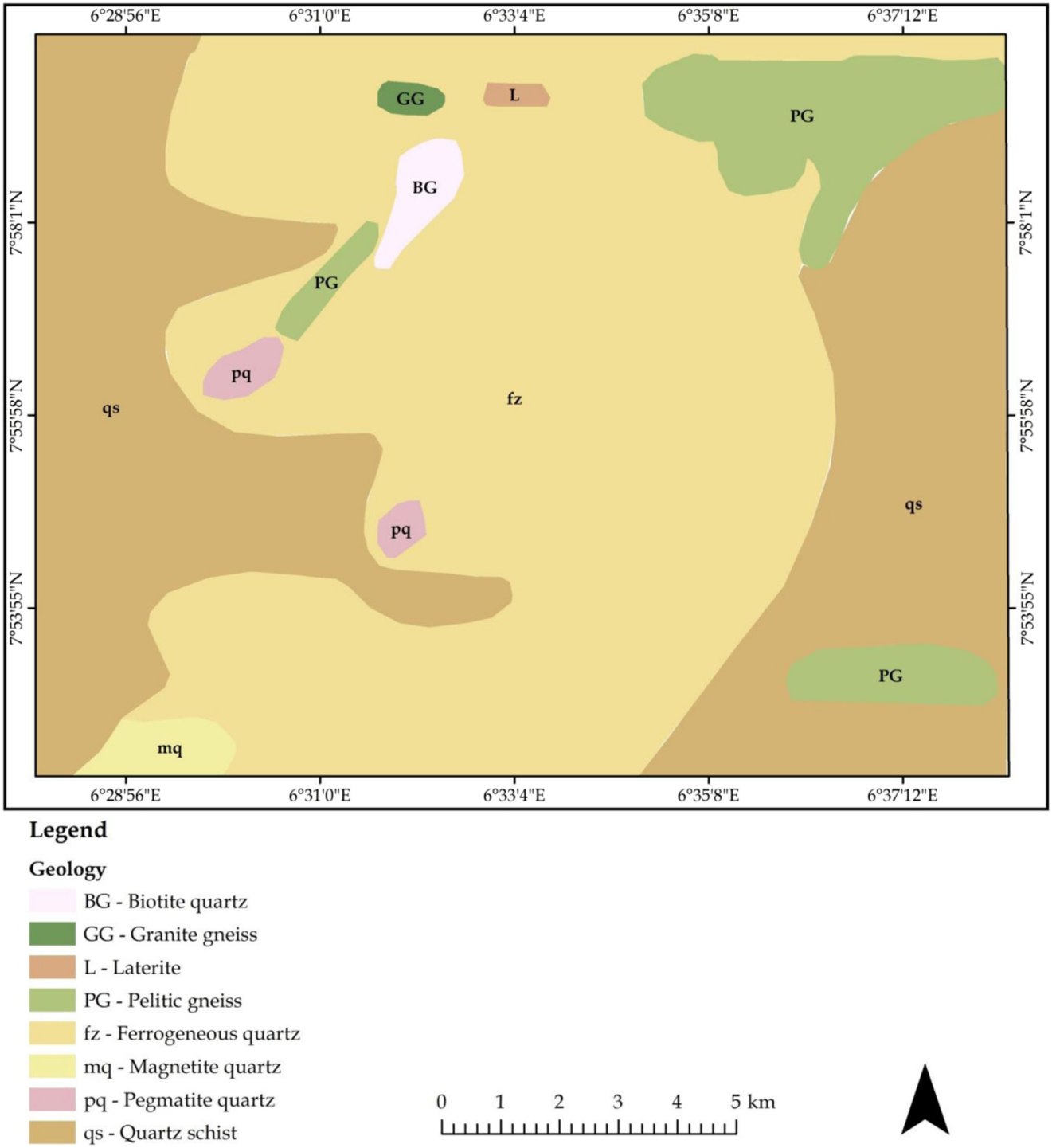


Fig. 2 Geology map of Agbado-Okudu iron ore deposit area

was recorded while the strike of the outcrop is essentially in the northwest–southeast. In the south and southwest quadrant of this area are boulders and pebbles of quartz (milky quartz) and occurrences of quartz veins striking roughly east–west. A fairly extensive outcrop of brecciated ferrugineous quartzite in laterite matrix seems to indicate some degree of intensive deformation in this area (Fig. 2).

Materials and methods

Data acquisition

The data acquisition involved vertical magnetic intensity (ΔZ) measurements and gravity readings using a digital magnetometer (model MFD-4 manufactured by Scintrex) and a LaCoste–

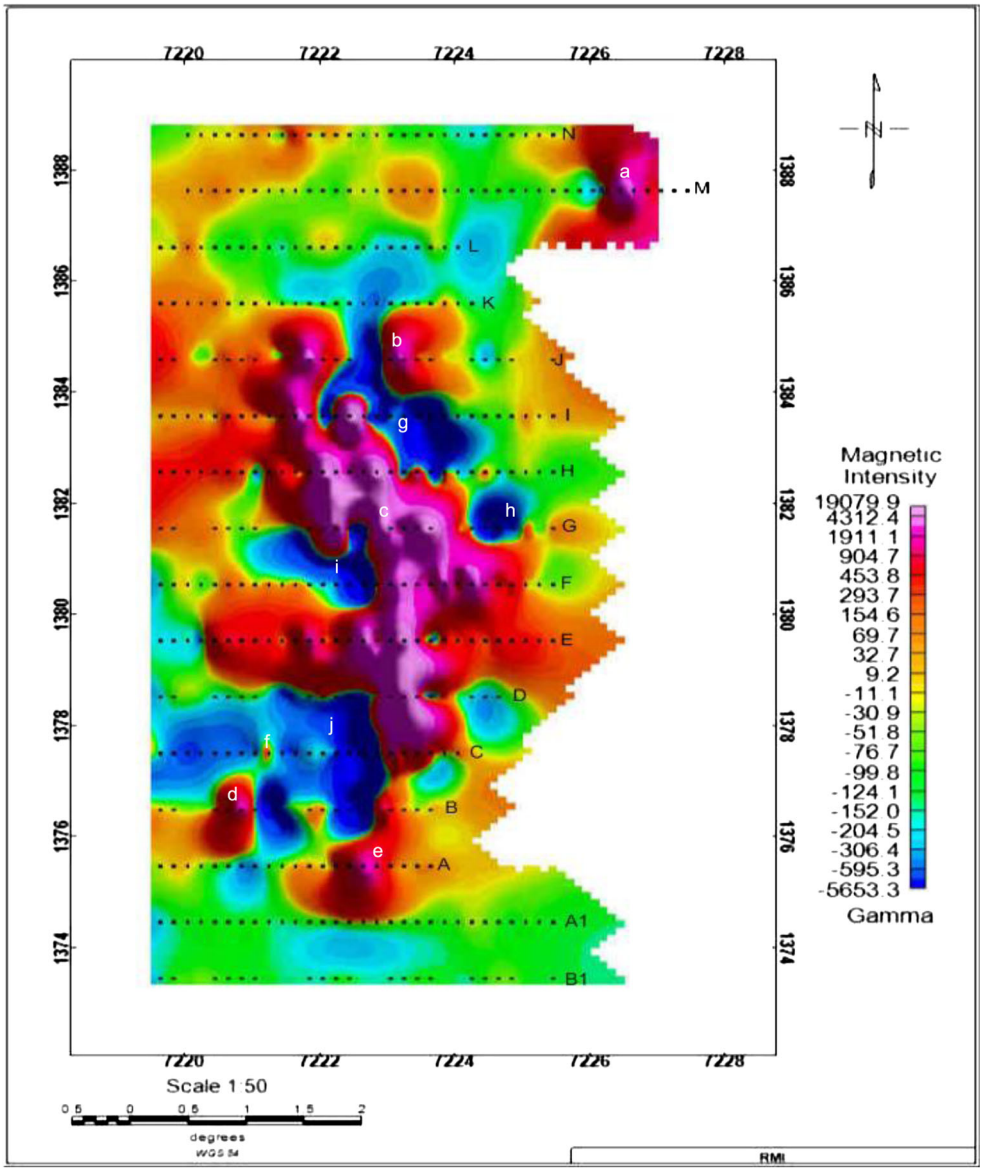


Fig. 3 Color-shaded residual magnetic intensity (RMI) map of the area, showing the anomalies (a, b, c…) along profiles (A1, B1, A…)

Romberg gravimeter. A total of 517 magnetic measurements along 16 profiles (B1, A1, A, B, …….M, N) and 330 gravity reading along 11 profiles (B1, A1, A, B, ….H, I) were undertaken (Fig. 3). The baseline established in the direction N 20° E coincided with the general trend and crest of the ridge. The profiles are spaced 100 m apart, normal to the baseline while the stations are spaced 40 m apart. The magnetic readings were taken in close loops of about 1 h repeated interval for diurnal variation correction. Field spot heights of each of the reading stations were obtained with Garmin etrex 10 global positioning system (GPS) and were used for coordinate projection and elevation correction. Traverses through the terrain were established with the aid of compass clinometers. The magnetic and gravity data were recorded profile by profile in Excel format and imported as ASCII (x, y, z) grid file format in Oasis montaj™ where x is the geographic longitude value; y as the geographic latitude value; with x and y in Universal Transverse Mercator (UTM), and z for magnetic intensity and gravity anomaly values.

Data processing

Potential field data of magnetic and gravity methods require certain processing and reductions in order to deduce meaningful interpretation and for improved data quality (Wynn 2002). Maps and images are derived from anomaly amplitude which is related to physical properties of the subsurface rocks, its structural features, and other desired parameters.

Magnetic data processing

Residual magnetic values for each station were obtained using a linear regression curve fitting for readings along each profile and

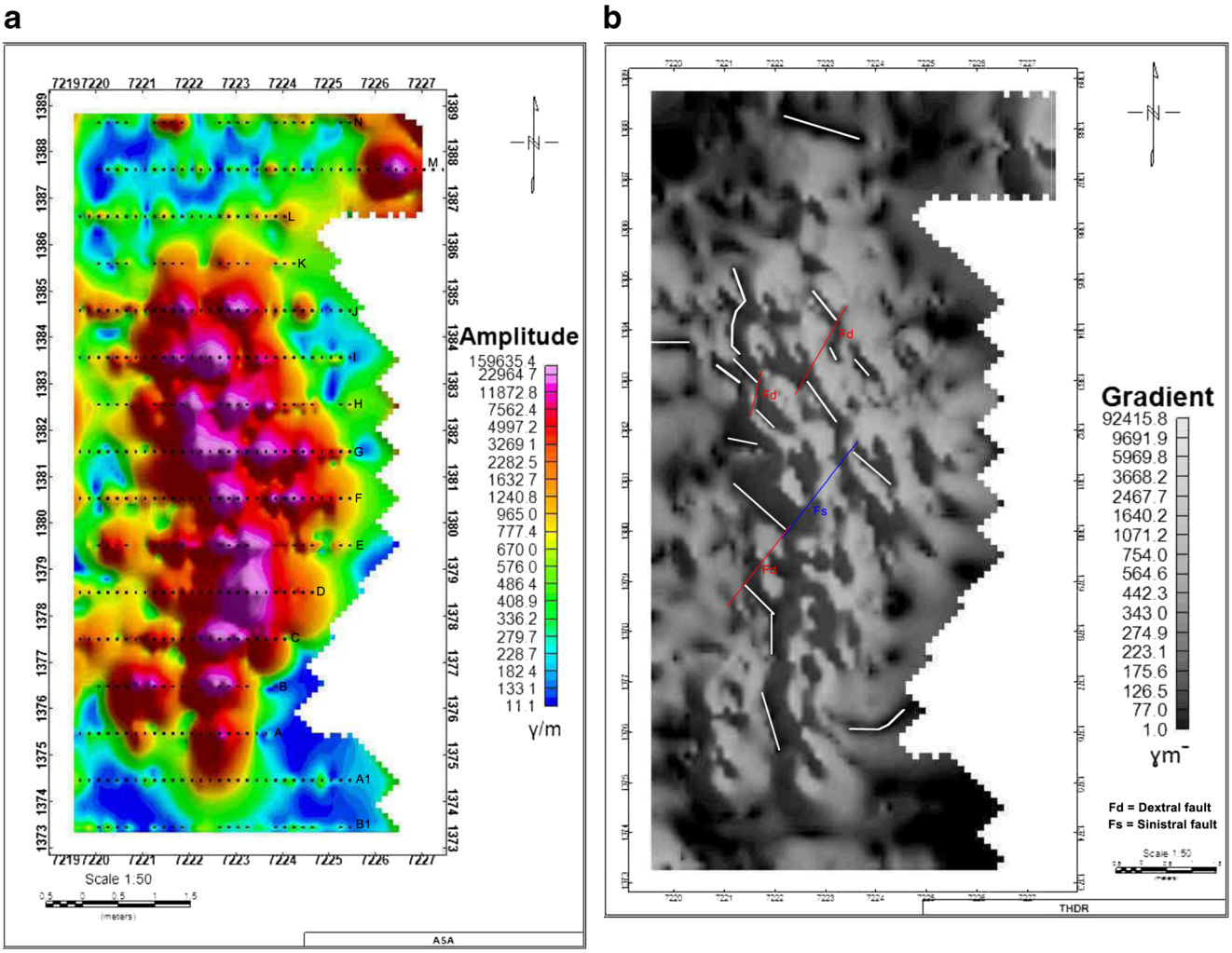


Fig. 4 Enhanced derivatives (**a**) color-shaded analytic signal amplitude and (**b**) gray-shaded total horizontal derivative of the residual magnetic intensity map

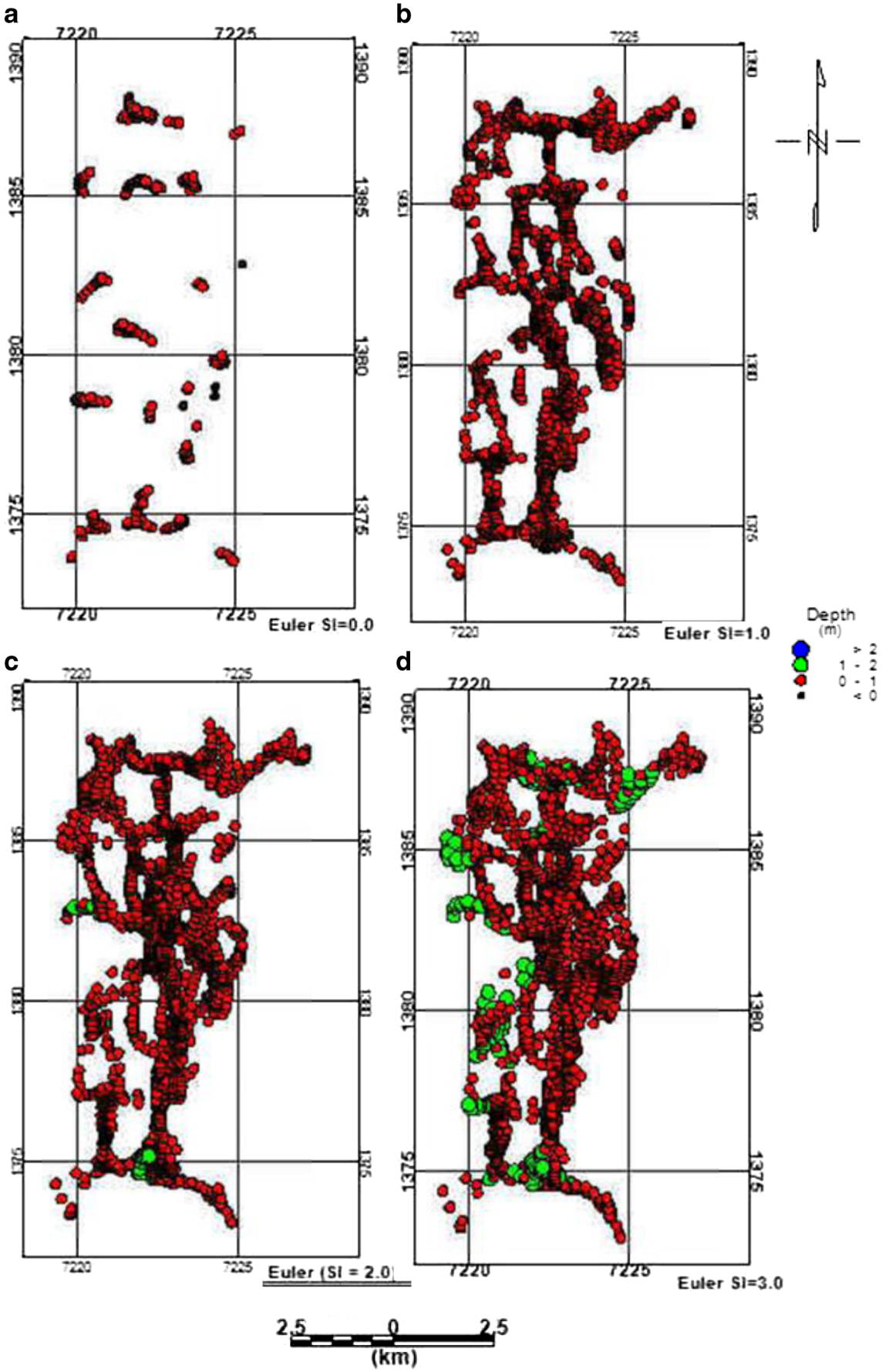
presented in Fig. 3. The residual magnetic values were plotted and subjected to various data filtering and processing tools involving analytic signal, Euler deconvolution at different spectral (SI), power spectrum, and source parameter imaging (SPI) using Geosoft Oasis Montaj 6.4.2 (HJ) software. The analytic signal (AS) was applied to delineate boundaries of intrusive bodies by producing maxima amplitude over the magnetic contacts regardless of direction of magnetization (MacLeod et al. 1993; Paananen 2013). It is also easily used to estimate the depth to sources from

Table 1 Structural indices (SI) for various geological models (adapted from Thompson 1982)

Geological model	Number of infinite dimensions	Magnetic SI
Sphere	0	3
Pipe	1 (Z)	2
Horizontal cylinder	1 (X or Y)	2
Dyke	2 (Z and X or Y)	1
Sill	2 (X and Y)	1
Contact	3 (X, Y and Z)	0

distance between inflection points of its magnetic anomalies. The theoretical details of this filter are covered by Blakely (1995) and Verduzco et al. (2004). The AS amplitude map produced from the residual anomaly is as depicted in Fig. 4a. Total horizontal derivatives (THDR) edge detection techniques were applied to amplify lineaments, which are structural deformations that are related to faults and other lateral changes or geological contacts. The gray color map of THDR is depicted in Fig. 4b. The prominent north–south trending dark tone shows definitive contact to the west between the schistose rocks and the ferruginous quartzite. Prominent northwest–southeast and some east–west lineament orientations are observed. These are in agreement with the Kibarian and Liberian orogeny cycles of deformation, metamorphism, and remobilization in Nigeria (Burke and Dewey 1972), respectively that are generally known structural trends in Nigeria.

Standard Euler uses the components of the analytic signal (three orthogonal derivatives) all in the spatial domain, usually determined by Fourier methods and has been applied for rapid depth estimation. It is designed to provide computer-assisted analysis of large volumes of magnetic data through the geometry of magnetic


a
b
c
d
7220
7225
1390
1385
1380
1375
Euler SI=0.0
Euler SI=1.0
Euler (SI = 2.0)
Euler SI=3.0
Depth
(m)
2.5 0 2.5
(km)

◀ **Fig. 5** Depth estimate with Euler deconvolution plot at different structural index obtained from the residual magnetic intensity map. **a** SI = 0.0. **b** SI = 1.0. **c** SI = 2.0. **d** SI = 3.0

bodies regarded as structural index and the governing equation as covered in Thompson (1982), Barongo (1984), Barbosa et al. (2000) and Reid (1997). The structural index is a measure of falloff rate of the field with distance from the source (Table 1) and could be used to locate or outline confined sources ($N=0$), vertical pipes and horizontal cylinder ($N=1$), intrusive bodies (thin layer, dyke, etc. $N=2$), and contacts ($N=3$) with remarkable accuracy by discriminate between different source shapes. The depth estimate obtained from Euler deconvolution is as shown in Fig. 5, and the corresponding radially average power spectrum is as in Fig. 6. For quick, easy, and automatic estimation of the source depth to corroborate that of Euler deconvolution and power spectrum, SPI was applied to the gridded data. The method estimates the depth from the local wavenumber of the analytic signal and requires second derivatives of the anomaly field, defined as the spatial derivative of the local phase (Nabighian 1972; Thurston et al. 2002; Salem et al. 2008). The resulting image is shown in Fig. 7.

Gravity data processing

The gravity readings were corrected for drift caused by the time-dependent mechanical changes within the LaCoste–Romberg gravimeter. The instrument drifts were computed between baseline ties, chosen to be the junction of Agbado-Okudu and the Lokoja-Jakura Marble Quarry Road at an elevation of 308.82 m. Elevation correction was done, using the World Geodetic System 1984 (*WGS 84*) on Geosoft Oasis Montaj 6.42 (HJ). Free air correction and Bouguer corrections were also applied for effect of masses lying between gravity point and the geoid's (Telford et al. 1990). The Bouguer anomally forms the basis for the interpretation of gravity data on land. The terrain correction could not be determined due to problem of accessibility in the study area, and its computation requires detailed knowledge of relief near all measured stations and topographic map (contour interval of 10 m or smaller) that extends considerably beyond the survey area (Dobrin and Savit 1988). A resulting gravity residual anomaly map (Fig. 8) was prepared from residual values obtained for each station using a second-order polynomial curve fitting along each of the gravity, and the corresponding magnetic anomalies and depth to magnetic sources are depicted in Fig. 9. Magnetic parameters $K.\tan^{-1}\left(\frac{b}{37.5}\right) = 0.3703$ and Kt = 16.34 have also been calculated using general equations for a dyke and thin sheet, respectively (Telford et al. 1976).

K	magnetic susceptibility
b	width of top of dyke

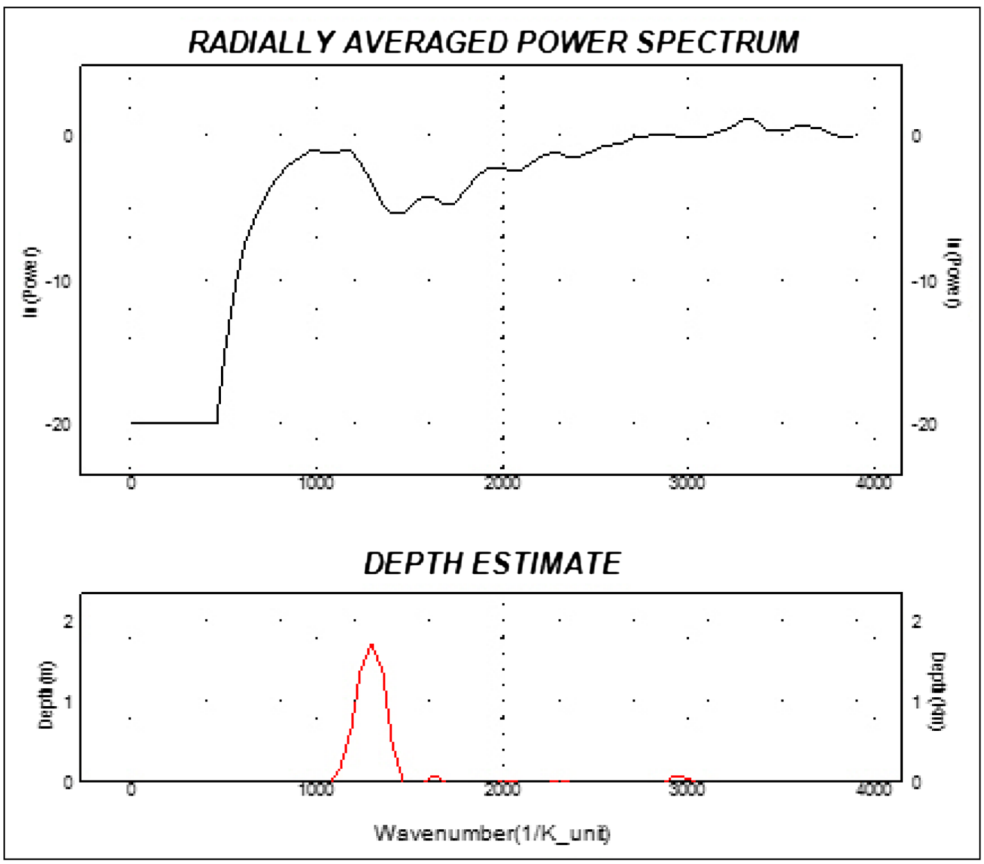


Fig. 6 Radially averaged power spectrum and depth estimate from spectral analysis plot of the area

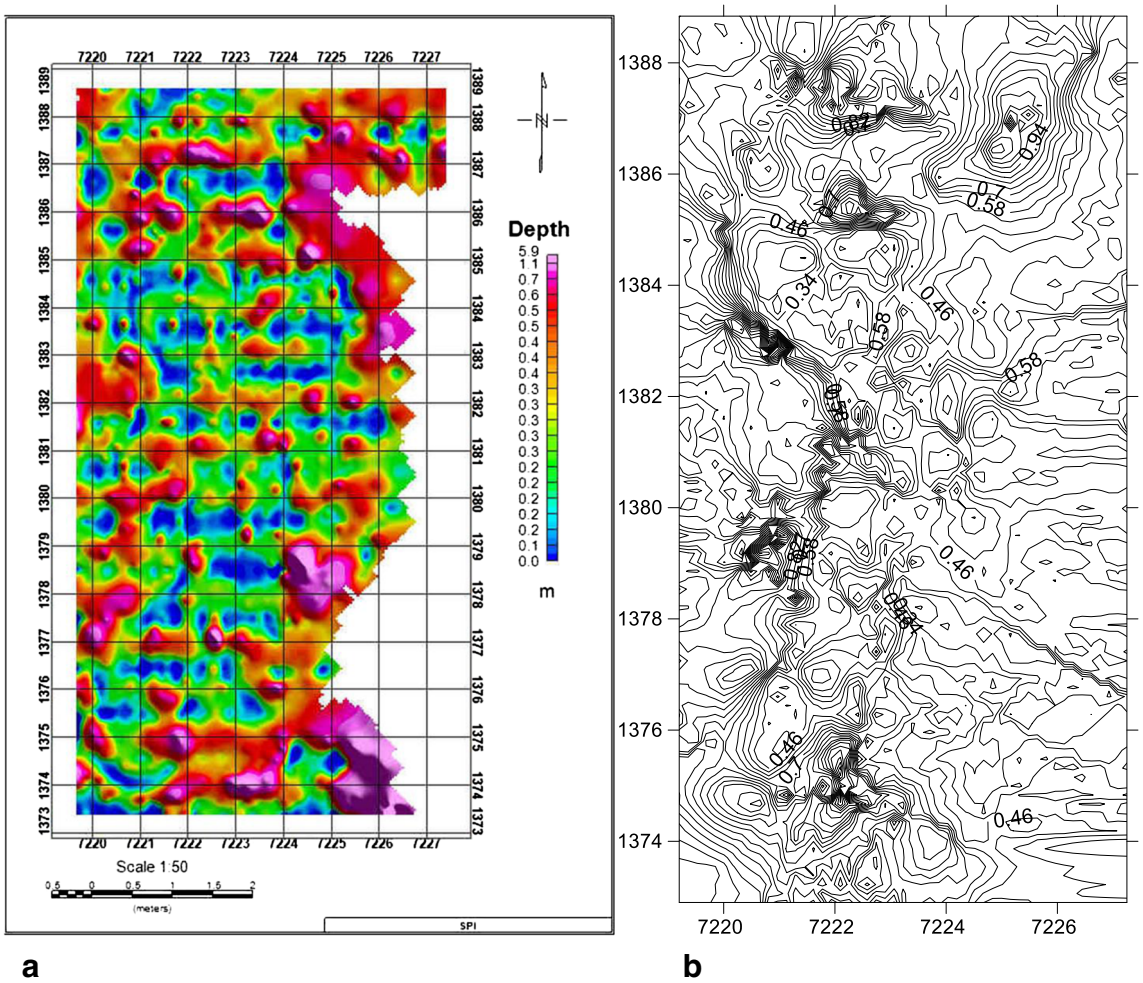


Fig. 7 Depth estimate plots. **a** Source parameter image. **b** Euler deconvolution at SI = 3 of the study area

t thickness of thin sheet

$\tan^{-1}\left(\frac{b}{37.5}\right)$ angle substended by top of dyke at the surface

Interpretations and discussion of results

Basement mapping

The color-shaded RMI map of the area shown in Fig. 3a revealed positive magnetic anomalies ranging from 9.2 to 19,079.9 gamma characterized the central, southern, and northeastern region; while negative magnetic anomalies ranging between − 11.1 and − 5653.3 gamma characterized the north central, eastern, and southwestern part of the map. It showed no significant modification of the original vertical magnetic anomalies. They are consistent in pattern, trend, and amplitude. A very close study of the RMI map revealed an alternating positive and negative magnetic values, which suggests contrasting rock types in the basement of the area, interpreted as two causative bodies for the anomaly recorded viz.; the primary cause depicted with pink–red color and marked anomalies a, b, c, d, and e, while the secondary causes are illustrated with blue–green color and marked g, h, i, and j anomalies. The primary cause is prominent and better emphasized, has a positive anomaly, strike roughly in the north–south azimuth, and is associated with the gneiss complex lithologic basement units. It coincided with the units represented on the geologic map as granite gneiss, biotite gneiss, and pelitic gneiss. The secondary causes are indicated by pockets of slightly elongated negative anomalies, suggesting the older granitoids and quartzitic intrusion, and trending northeast–southwest orientation. The iron ore outcrops perfectly correlate with the area of positive magnetic anomalies and region of high gravity anomalies in the color-shaded anomaly map (Fig. 8). The gravity anomaly ranged from − 15.5 to − 1.7 mgal, and its corresponding sections (Fig. 9) showed three major anomaly categories; types A, B, and type C. The type A and B anomalies trend roughly N–S and NE–SW, respectively which correlate with the primary and the secondary causative bodies, recognized from the magnetic map (Fig. 4). The anomaly type C, which is roughly circular to oblate in the NW corner of the map, and the A type in the SW and SE corners of the map are very poorly reflected on the magnetic map.

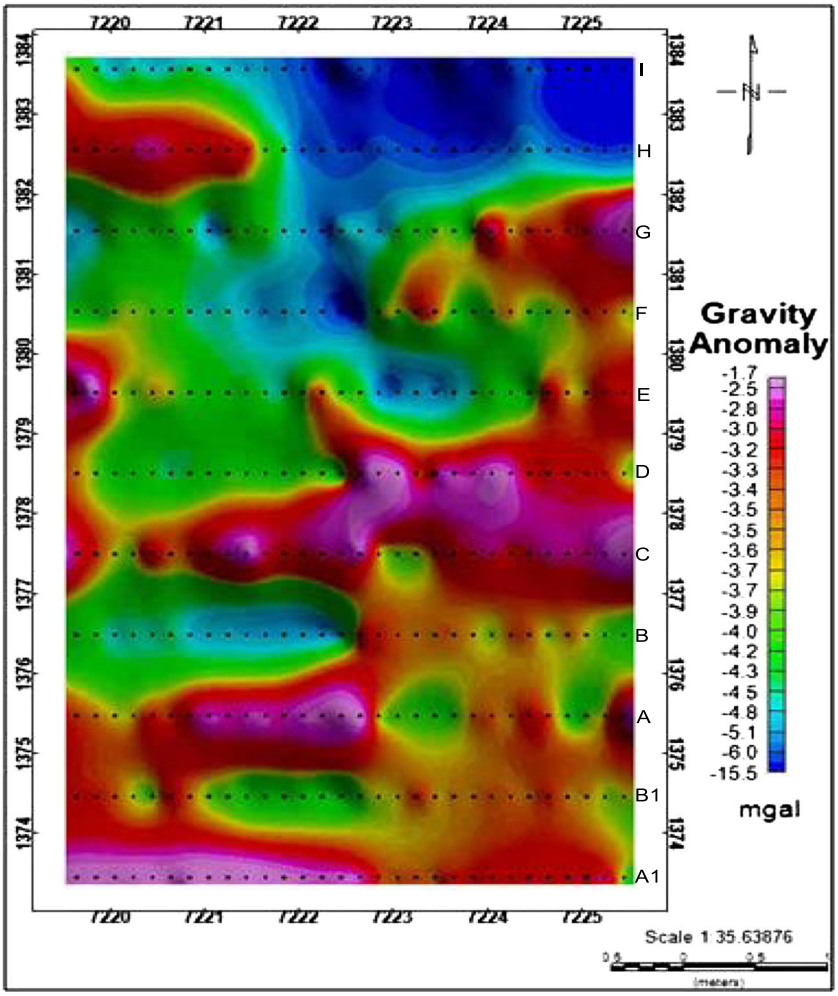


Fig. 8 Color-shaded residual gravity map showing gravity anomalies of the study area

Depth to basement

The Euler results from the magnetic data analysis showed in Fig. 5 revealed that the SI = 0, 1, 2, 3 are solutions for the modeled geologic features as there are tightest clusters along some notable anomalies inferred to make the ore outcrops in the central, southern, and northeastern corner of the study area. The estimated depth to basement around Agbado-Okudu iron ore from Fig. 5 ranged between ≤ 0.0 and ≥ 2.0 m. Possible depth solutions from the Euler deconvolution correspond to basement rock contact, intrusive bodies (sill/dyke), horizontal cylinder, and sphere geological model (Table 1). The radially average power of spectral analysis in Fig. 6 showed average depths of source assemblage as ≤ 2.0 m while the source parameter imaging technique estimated the depth range between 0.0 and 6.0 m. Calculated depth from gravity anomaly (type A) in the profiles A and I (Fig. 9) range within 37.5 ± 11.25 m or 50 m and 45 ± 13.50 m or 60 m and assuming their responses to be that a vertical thin rod or horizontal cylinder. Profile D showed anomaly type C, which indicates the response of a semi-infinite horizontal sheet (or a faulted half plane) and has been calculated to have a thickness of about 24 m. This corresponds to the estimated depth of ≥ 50.0 m and correlates with the result of Euler deconvolution.

Structural framework

The suitability of total horizontal derivative and analytic signal amplitude for mapping contacts of vertical bodies at maximum amplitude has been established (Fairhead et al. 2007; Salem et al. 2008; Paananen 2013). The lineament that revealed the subsurface features was extracted from the THDR map (Fig. 10) using Surfer 11 Geosoft and shows prominent (79%) NW–SE orientation and some (21%) E–W orientation. The lineaments were superposed on the residual magnetic map (Fig. 10), and displacement in the linear features revealed the block rotation in clockwise and anticlockwise directions, which has been interpreted as dextral and sinistral faults, respectively. The faults correlate with the lateral displacement inferred from break in continuity of the relatively low positive anomaly values, enclosed in the roughly parallel zero contour lines between profiles B, C, and D in southern part of the area.

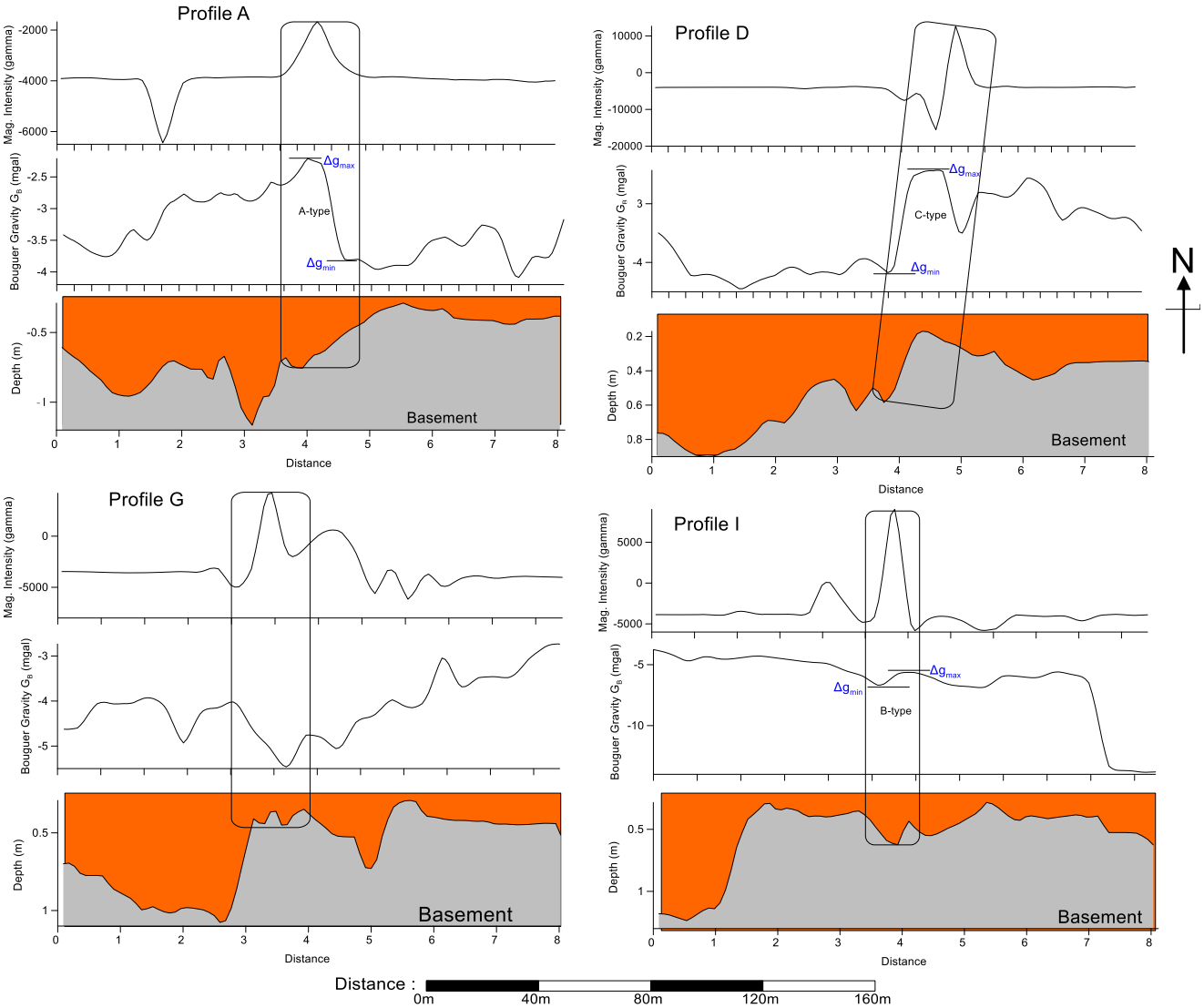


Fig. 9 Modeled profiles and estimated depths along the iron ore deposit showing sections across magnetic and gravity anomalies

The variation in the magnetization of the magnetic sources, highlights of discontinuities, and anomaly texture were accentuated by the analytical signal derivative map (Fig. 4a), which indicates that the lineaments are within shallow sources with high amplitude range between 7562.4 and 159,635.4 ɣ/m.

The gravity anomaly on profile G (Fig. 9) is a representative section across the probable primary causative bodies which has been inferred to indicate the response of a horizontal or very gentle dipping (towards the East) dyke with a strike length of about 600 m. On top of this dyke, the width ranges from 110 to 130 m. The section on profile I with its two prominent positive peaks also indicates a response of two bands of horizontal or gently dipping dykes. Anomaly section on profile D (Fig. 9) belongs to the secondary causes and has been taken to represent a vertical or near vertical sheet (or dyke) with an infinite depth extent. A depth (to top) of 37.5 m (if a dyke) and depth range of 41.67–46.86 m (if a sheet) have been calculated for this body.

Conclusions

A combined interpretation of the magnetic and gravity data obtained at Agbado-Okudu has been attempted using manual analysis and Geosoft Oasis Montaj 6.4.2 (HJ) data processing and analysis software. The results of the interpretation revealed the distribution of concealed iron ore formation, depth to magnetic sources, basement structures, boundaries, and lithologic contacts within the study area. The contrasting magnetic values from the residual magnetic intensity ranging between 9.2 to 19,079.9 gamma and − 11.1 and − 5653.3 gamma revealed two possible causative bodies; the primary cause which is prominent and better emphasized has a positive anomaly, associated with various basement rock types; and the secondary causes which are indicated by pockets of slightly elongated negative anomalies, associated with pegmatitic and quartzitic intrusion.

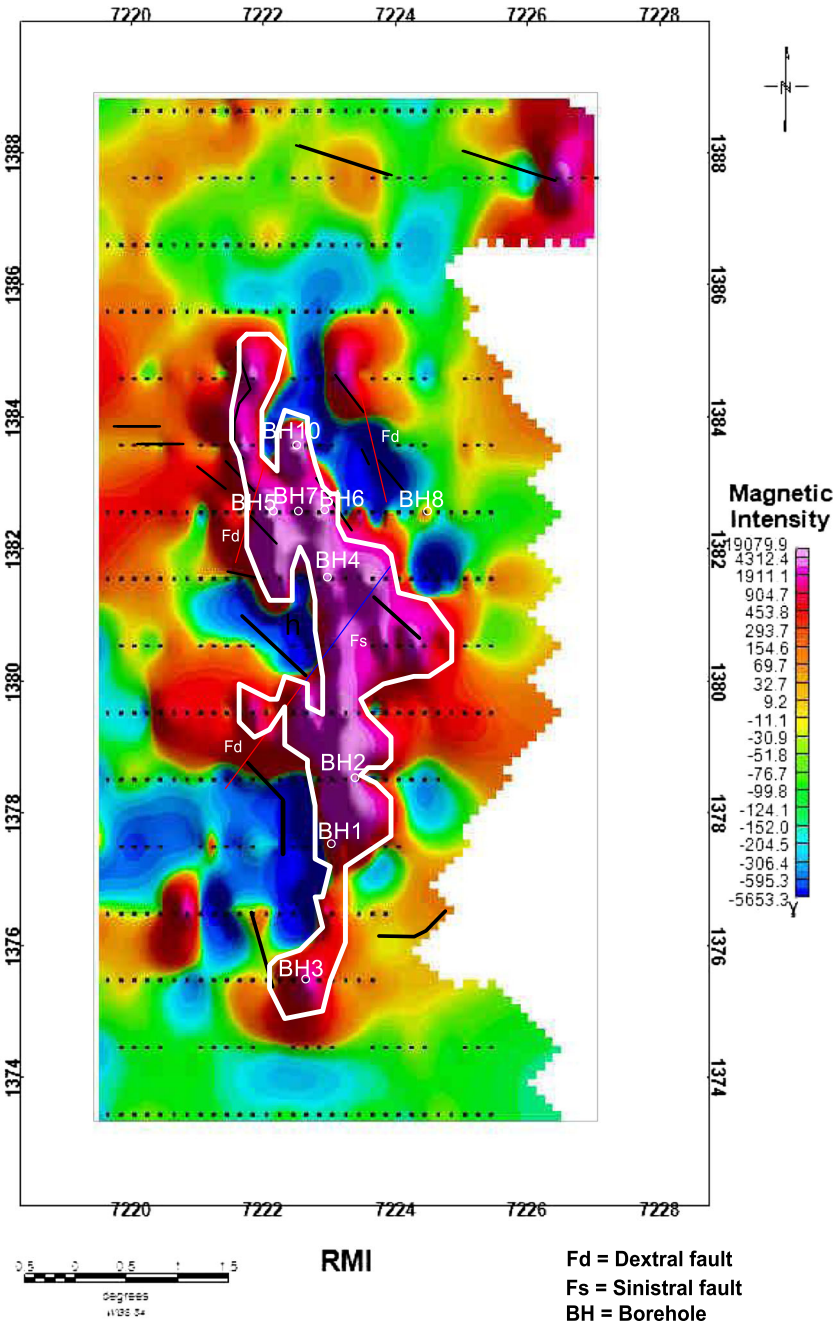


Fig. 10 Magnetic lineament classification and faults map of the study area

The iron ore outcrops perfectly correlate with the area of positive magnetic anomalies and fault geologic features obtained through lineaments extracted from the total horizontal derivative map. The gravity anomalies indicate the iron ore outcrop as a horizontal or gently east dipping dyke, distributed within the north-eastern, north central, to southern portion of the study area and existing at shallow depth range of ≤ 2 to 24 m and relatively deep range of 37.5 to 60 m.

The mode of occurrence and associated geologic features of Agbado-Okudu iron ore formation has been deduced from the analysis and interpretation of its magnetic and gravity data. In the light of the foregoing, vertical boreholes are recommended with depth range of 50–100 m at BH1 around 720 m on profile C, BH2 at 1040 m on profile D, BH3 at 640 m along profile A, BH4 at 720 m along profile G, BH10 at 400 m on profile I, and BH5, BH6, and BH7 at 760 m, 1080 m, and 1160 m on profile H, respectively. A borehole at 760 m on profile F is recommended to determine the depth to the top of the secondary causative body which has been calculated to be between 41.6 and 46.88 m while BH6, BH7, and BH10 have been recommended to establish the cause of the anomalies indicated at the SW, SE, and NW corners of the gravity map.

References

Amigun JO, Afolabi O, Ako BD (2012) Application of airborne magnetic data to mineral exploration in the Okene Iron Ore Province of Nigeria. Int Res J Geology Min (IRJGM), 132–140.

Barbosa VCF, Silva JBC, Medeiros WE (2000) Making Euler deconvolution applicable to small ground magnetic surveys. J Appl Geophys 43:55–68

Barongo JO (1984) Euler's differential equation. Geophysics, 1549–1553

Blakely RJ (1995) Potential theory in gravity and magnetic applications. Cambridge Univ. Press, Cambridge

Burke KC, Dewey JF (1972) Orogeny in Africa. In: Dessauvagie TF, Whiteman AJ (eds) Africa geology. University of Ibadan Press, Ibadan, pp 583–608

Cericia M, Yaoguo L, Richard K, & Marco B (2011) Lithologic characterization using magnetic and gravity gradient data over an iron ore formation. SEG San Antonio 2011 Annual Meeting (pp. 836–840). San Antonio: SEG

Dobrin MB, Savit CH (1988) Introduction to geophysics prospecting. McGraw-Hill Book Co. Inc., New York

Durrheim RJ (1983) Regional-residual separation and automatic interpretation of aeromagnetic data:. Unpublished M.Sc. thesis, University of Pretoria, 117

Emerson DW (1990) Notes on mass properties of rocks—density, porosity, permeability. Explor Geophys, 209–216

Fairhead D, Williams S, Ben SA (2007) Structural mapping from high resolution aeromagnetic data in Namibia using normalized derivatives. Innovation in EM, Grav and Mag methods: a new perspective for exploration. EGM 2007 International Workshop, Capri

Foss C (2011) Magnetic data enhancement and depth estimation. In: Gupta HK (ed) Encyclopedia of Solid Earth Geophysics. Springer Science + Business Media B.V, Dordrecht

Hansen DA (1966) The search for iron ore—ore classification susceptibility geophysical methods. SEG Min Geophysics, 359–364

Macleod IN, Jones K, Fan Dai T (1993) 3-D analytic signal in interpretation of total magnetic field data at low magnetic latitudes. Explor Geophys 24:679–688

Nabighian MN (1972) The analytic signal of two-dimensional magnetic bodies with polygonal cross-section: its properties and use for automated anomaly interpretation. Geophysics 37:507–517

Obaje GN (2009) Geology and mineral resources of Nigeria. Springer-Verlag Berlin Heidelberg, London New York

Oladunjoye MA, Olayinka AI, Alaba M, Adabanija MA (2016) Interpretation of high resolution aeromagnetic data for lineaments study and occurence of banded iron formation in Ogbomoso area, Southwestern Nigeria. J Afr Earth Sci 114:43–53

Paananen M (2013) Complete lineament interpretation of the Oikiluoto region. Posiva, 2013–02 ISBN 978–951–652-234-3

Rahaman MA (1989) Review of basement geology of South-Western Nigeria. In: Kogbe CA (ed) Geology of Nigeria. Elizabeth Publ, Lagos, pp 41–58

Reid AB (1997) Euler deconvolution, past, present and future "Proceedings of Exploration 97:" edited by A.G. Gubins, p. Fourth Decennial International Conference on Mineral Exploration, (pp. 861–864)

Salem A, Williams S, Fairhead D, Smith R, Dhananjay R (2008) Interpretation of magnetic data using tilt-angle derivatives. Geophysics 73:L1–L10

Spector A, Grant FS (1970) Statistical models for interpreting aeromagnetic data. Geophysics 35:293–302

Telford WM, Geldart LP, Sheriff RG, Keys DA (1976) Applied Geophysics. Cambridge University Press, Cambridge

Telford WM, Geldart LP, Sheriff RE, Keys DA (1990) Applied geophysics. Cambridge University Press, Cambridge

Thompson DT (1982) EULDPH-new technique for making computer-assisted depth estimates from magnetic data. Geophysics 47:31–37

Thurston JB, Smith RS, Guillion JC (2002) A multi-model method for depth. Geophysics 67:555–561

Verduzco B, Fairhead JD, Green CM, MacKenzie C (2004) New insights into magnetic derivatives for structural mapping. Lead Edge 23: 116–119

Wynn J (2002) Evaluating ground water in arid lands using airborne electromagnetic methods—an example in the southwestern U.S. and northern Mexico. Lead Edge, 62–65